[CANCER RESEARCH 64, 6247–6251, September 1, 2004]

Detection of Invasive Colon Cancer Using a Novel, Targeted, Library-Derived Fluorescent Peptide

Kimberly Kelly, Herlen Alencar, Martin Funovics, Umar Mahmood, and Ralph Weissleder

Center for Molecular Imaging Research, Department of Radiology, Massachusetts General Hospital and Harvard Medical School, Charlestown, Massachusetts

ABSTRACT

Sensitive methods to detect the earliest forms of colorectal cancers remain a challenge despite the development of serum and stool biomarkers. We reasoned that fluorescent affinity ligands derived from library screens can be developed to improve the detection and localization of early malignant lesions by endoscopy. We have developed an imaging agent for real-time endoscopic tumor detection in a murine model using a previously identified phage library-derived colon cancer-specific cyclic peptide and fluorescent moieties. The modified peptide had a 24 minute blood half life and tumoral accumulation was 6.9% of injected dose/g, ~7-fold higher than a scrambled control peptide. Orthotopic colonic tumors (HT29) were readily detectable by fluorescence endoscopy even when tumors were submucosal. These results show proof-of-principle that disease-specific library-derived fluorescent probes can be rapidly developed for use in the early detection of cancers by optical means.

INTRODUCTION

Colorectal carcinogenesis is a stepwise process involving a transition from normal mucosa to the development of cancer and is the end result of a series of molecular alterations (1), environmental influences, and host responses over time (2). The process of carcinogenesis can take years, theoretically providing opportunity for life-saving diagnosis and treatment. Unfortunately, colorectal cancer still remains a significant cause of death in the United States because it often remains undetected until later stages of the disease (3). Screening endoscopy with routine polypectomy is widely used and has been shown to reduce the incidence of colorectal cancer (4). Despite these advances in screening, routine endoscopy has been reported to have miss rates of early adenomas of up to 20% (5). This rate increases substantially in subsets of lesions that do not originate in polyps (flat lesions; refs. 6, 7), lesions that arise in polyposis syndromes (8), or lesions in inflammatory bowel disease such as Crohn's disease and ulcerative colitis (9).

Novel endoscopic tools are currently being developed to increase the accuracy of early cancer detection in the gastrointestinal tract. Recently, we have developed miniaturized multichannel near-infrared fluorescence endoscopes for mouse imaging (10) and shown that near-infrared fluorescence endoscopy in conjunction with near-infrared fluorescence imaging probes specific for tumor cells can improve the detection of adenomas in APCmin mice (11). Here, we show that differential phage display peptide motifs can be converted into high-affinity imaging agents for optical cancer detection. We specifically show that a modified near-infrared fluorescence agent containing a cyclic RPMC peptide motif can be used to detect invasive colorectal cancer by near-infrared fluorescence endoscopy in a mouse model.

Received 3/5/04; revised 5/19/04; accepted 5/21/04.

Grant support: NIH Grants CA86355 (R. Weissleder), CA92782 (R. Weissleder, U. Mahmood), and EB02102 (K. Kelly).

The costs of publication of this article were defrayed in part by the payment of page charges. This article must therefore be hereby marked *advertisement* in accordance with 18 U.S.C. Section 1734 solely to indicate this fact.

Requests for reprints: Ralph Weissleder, Professor, Harvard Medical School, Director, Center for Molecular Imaging Research, Massachusetts General Hospital, Harvard Medical School, 149 13th Street, Room 5404, Charlestown, MA 02129. Phone: (617) 726-8226; Fax: (617) 726-5708; E-mail: weissleder@helix.mgh.harvard.edu.

MATERIALS AND METHODS

Materials. DMEM, McCoy's medium, 1 mol/L HEPES solution, sodium pyruvate solution, sodium bicarbonate solution, Dulbecco's PBS with Ca^{2+} and Mg^{2+} ($DPBS^{+}$), and HBSS were purchased from Biowhittaker Bioproducts (Walkersville, MD). FCS was purchased from Cellgro (Herndon, VA). Dota-tris(t-butyl)ester was purchased from Macrocyclics (Dallas, TX). ^{111}Indium chloride in 0.05 mol/L HCl was purchased from Perkin-Elmer Biosciences (Boston, MA). Amino acids for peptide synthesis were purchased from NovaBiochem (La Jolla, CA). All other chemicals were of the highest quality grade available from Fisher Scientific (Suwanee, GA) or Sigma Chemical Co. (St. Louis, MO).

Cell Culture. All cells were obtained from the American Type Tissue Culture Collection (Manassas, VA). The HT29 cell line was maintained in McCoy's medium supplemented with 10% FCS, 2 mmol/L L-glutamine, and 1 mmol/L sodium pyruvate at 37°C in 5% CO_2. CT 26 cells were maintained in DMEM supplemented with 10% FCS, 2 mmol/L glutamine, and 1 mmol/L sodium pyruvate at 37°C in 5% CO_2. For routine maintenance, cells were passaged by trypsinization immediately upon reaching confluence.

Murine Models. C57Bl/6 wild-type mice (7 to 9 weeks) were purchased from Taconic (Germantown, NY), and nude mice were purchased from COX-7. All mice were maintained in approved pathogen-free institutional housing facilities. All experiments were performed according to institutional guidelines. Animals were sacrificed by carbon dioxide asphyxiation as approved by the panel on Euthanasia at the American Veterinary Association.

Synthesis of Peptide Conjugates. The peptide sequence 'CPIEDRPMC' identified by phage display was extended at the COOH terminus by the sequence 'GGSK' to provide attachment points for fluorochromes (e.g., FITC, Cy 5.5) or for the macrocyclic chelator 1,4,7,10-tetraazacyclododecane-*N*,*N*′,*N*″,*N*‴ -tetraacetic acid (DOTA). FITC makes an ideal fluorochrome for in vitro assays and in vitro experiments because it is inexpensive, easy to chemically incorporate, and can be used for sensitive, quantitative measurements using an ELISA-based assay (12). Near-infrared fluorescence such as Cy5.5 on the contrary are better suited for in vivo imaging because it is resistant to photobleaching, and autofluorescence is much lower at this wavelength. The COOH-terminal lysine of the peptide was protected by 1,1-di(p-chlorophenyl)-2,2-dichloroethylene on the side chain to allow easy removal and conjugation of the peptide to either fluorochrome for optical imaging or DOTA for isotope chelation. All peptides were synthesized on an ACT APEX 396 peptide synthesizer using standard FMOC chemistry. FITC or Cy5.5-NHS was reacted with the resin bound peptide in DMSO/N,N-diisopropylethylamine overnight. DOTA was conjugated to resin bound peptide under standard amino acid reaction conditions using 3,3-tetramethyluronium hexafluorophosphate as a coupling agent and collidine as a base. Peptides were cleaved with reagent L (8.8 mL of trifluoroacetic acid, 500 mg of DTT, 500 mL of triisoprpyl silane, and 1.2 mL of H_2O) and purified by high-performance liquid chromatography. The peptide was then cyclized via S-S linkage by overnight reaction in ammonium bicarbonate (0.1 mol/L, 4°C, pH 8.0), as suggested by NovaBiochem (2004/05 catalogue, Method 3-38), lyophilized, and verified by mass spectral analysis. To radiolabel peptides, DOTA conjugated peptides were incubated with ^{111}InCl (Perkin-Elmer Biosciences) in 0.1 mol/L sodium acetate (pH 8.0) overnight at 37°C. After incubation, radiolabeled peptide was purified by size exclusion chromatography using P2 Biogel (Bio-Rad). The following compounds were synthesized in bulk: RPMC-F, CPIEDRPMCGGSK(F) where F = FITC or Cy5.5; REPC-F (control), CMPDIREPCGGSK(F) where F = FITC or Cy5.5; RPMC-DOTA, CPIEDRPMCGGSK(DOTA)^{111}In; and REPC-DOTA (control), CMPDIREPCGGSK(DOTA)^{111}In.

Fluorescence Microscopy. Confluent HT29 cells were incubated with 10 μmol/L of either RPMC-F or REPC-F for 1 hour at 4°C or 37°C, washed three times with PBS, and then visualized by fluorescence microscopy (×40 objec-

tive, Nikon Eclipse TE2000-S, Insight QE; Nikon, Melville, NY) or confocal microscopy (×40 objective, Olympus Fluoview; Olympus, Melville, NY).

$\alpha_5\beta_1$ Binding Experiments. Competition with human fibronectin was performed by coincubating HT29 cells with 10 μmol/L RPMC-F with 100 μmol/L fibronectin for 1 hour at 37°C. Quantitation of FITC was done by ELISA immunoassay (12). To determine whether RPMC-F bound to $\alpha_5\beta_1$, 10 μg of purified $\alpha_5\beta_1$ (Chemicon, Temecula, CA) was immobilized on Nunc Maxisorp immunoplates (Fisher Scientific), blocked with PBS/0.1% BSA, then incubated for 1 hour at 37°C with 5 μmol/L RPMC-F or REPC-F. After incubation, wells were washed six times with PBS/0.1% BSA/0.1% Tween 20 then fluorescence was read on a fluorescence plate reader (Gemini XS; Molecular Devices, Sunnyvale, CA). For competition experiments, HT29 cells were incubated for 1 hour at 37°C with RPMC-F (5 μmol/L) or RPMC-F (5 μmol/L) that was preincubated with $\alpha_5\beta_1$ (50 μmol/L). HT29 cells were then detached and analyzed via flow cytometry (10,000 cells per sample) on a Becton Dickinson FACSCalibur (San Jose, CA).

Primary Tissue Analysis. For binding of RPMC-F to *ex vivo* tissue sections, multiple human biopsy samples were snap frozen, embedded in OCT, cut into 5-μm sections, and then arrayed on slides. The tissue microarrays containing both colon adenocarcinoma and normal colonic tissue were incubated with 10 μmol/L RPMC-F for 1 hour at 37°C, washed three times with PBS, fixed with 2% paraformaldehyde, and then visualized by fluorescence confocal microscopy (×40 objective; Olympus Fluoview). To test the specificity of the peptide interaction with the tissue sections, slides were coincubated with 10 μmol/L RPMC-F with either 100 μmol/L unlabeled RPMC or REPC for 1 hour at 37°C. Nuclei were stained in the last wash by the addition of TOPRO-3 (Molecular Probes, Eugene, OR).

Tissue Distribution. The biodistribution of the labeled RPMC peptides was studied in nude mice bearing s.c. implanted tumors derived from the immortalized human colon cancer cell line HT29. Mice were anesthetized with 80/12 mg/kg ketamine/xylazine, and the radioligands (100 μCi) or radioligand with cold competitor (6 mg/kg) were injected into the tail vein. Scintographic images were obtained immediately, 30, 60, 90, 120, and 240 minutes after injection using a medium field of view gamma camera equipped with a medium energy collimator and controlled by Siemens Icon software (Siemens M-cam; Siemens Corp., Munich, Germany). Heart rate, oxygen saturation, and temperature of the animals were monitored during the experiment. The mice were sacrificed 4 or 24 hours after administration of the radiopeptide, and organs were harvested for biodistribution experiments. Radioactivity was determined in the injectate, tissues, and blood using a Wizard-3 1480 Automatic Gamma Counter (Perkin-Elmer Biosciences). The data are expressed as the % of injected dose/g (% ID/g; means ± SD).

Fluorescence Endoscopy. Nude mice were injected subcutaneously with 1×10^6 CT 26 colon cancer cells. When the tumor reached a 7–10-mm size, the mice were sacrificed, and the tumor resected and kept in cold saline solution for implantation. Immediately after tumor resection, a second set of nude mice were anesthetized with isoflurane and operated under a surgical microscope (Leica). An abdominal midline incision was performed, and the descending colon was identified. A 4-mm opening was created longitudinally in the colon, and a 4 × 2 × 2-mm tumor piece was sutured in a water-tight fashion using a 7-0 prolene running suture sealing the opening. The abdominal wall was closed in a two layers fashion with a 5-0 prolene running suture.

Seven days after tumor implantation, the mice were submitted to a colonoscopy examination under isoflurane anesthesia using a two channel fiberoptic microendoscope (10). The RPMC-F peptide was injected i.v. 2 hours before the colonoscopy. Both white light and infrared images were acquired simultaneously (10).

Histology. Immediately after endoscopic evaluation, the colons were removed, fixed in 2% paraformaldehyde, embedded in OCT, snap frozen, and serial sectioned (10 μm). One section was stained with H&E while the adjacent section was mounted with Vectashield (Vector Laboratories) and analyzed by fluorescence microscopy. Digital images were taken using an Axiovert-100-TV upright microscope (×40 objective) equipped with a DAGE-MTI CCD100 camera.

RESULTS

Affinity Ligands. Fig. 1*A* shows a model of the cyclic peptide motif RPMC previously identified by phage display (13) and now converted into a functional imaging agent by COOH-terminal extension bearing FITC or the near-infrared fluorochrome Cy5.5. The peptide cyclized rapidly, even at pH 7.4, as determined by high-performance liquid chromatography. COOH-terminal modification of the peptide with the GGSK motif containing FITC, Cy5.5, or DOTA did not affect the specificity toward HT29 cells as determined by fluorescence microscopy (Fig. 1*B*) and Scatchard analysis. The bind-

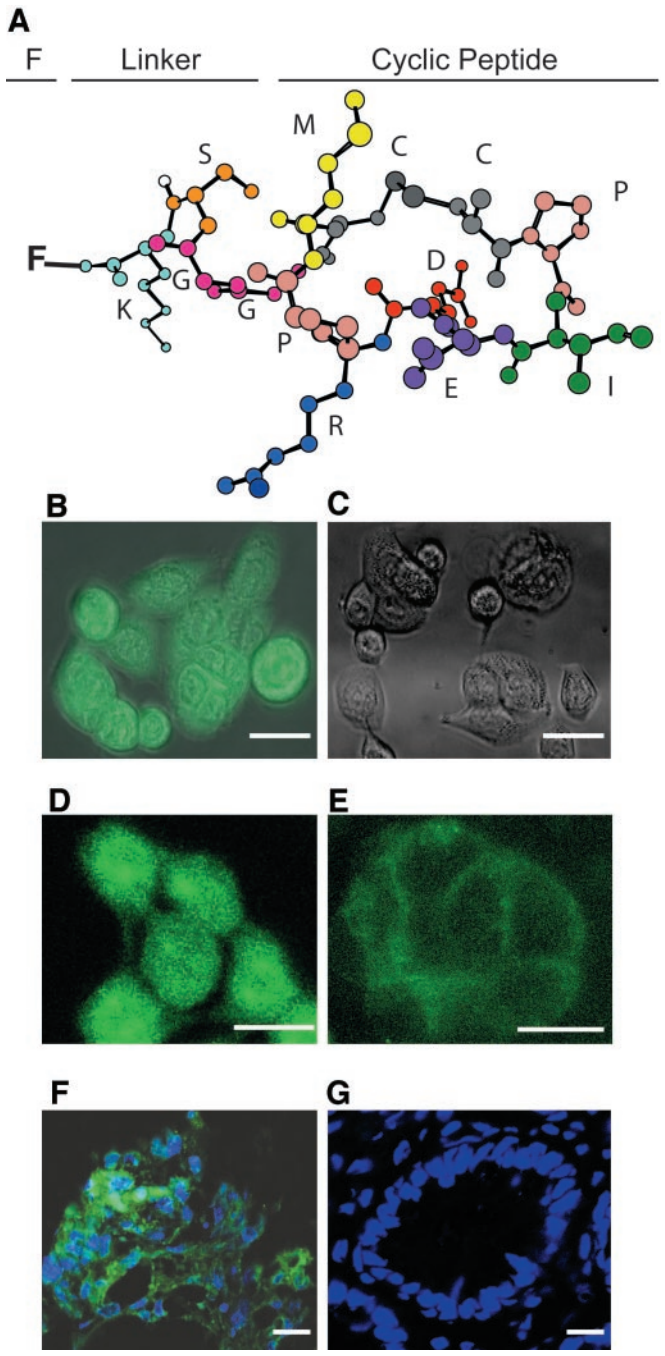

Fig. 1. RPMC peptide targets colon cancer. *A*, model of the cyclic RPMC peptide. Each amino acid is represented in a different color. HT29 cells were incubated with either RPMC-FITC (*B*) or REPC-FITC (*C*). Peptide binding was analyzed by fluorescence microscopy (×40) and overlaid with corresponding phase contrast micrographs. HT29 cells were incubated with RPMC-F at 37°C (*D*) or 4°C (*E*), then analyzed by fluorescence confocal microscopy. Note the RPMC-F specificity and internalization into HT29 cells. Representative examples of colon cancer (*F*) and normal colon tissue (*G*) from tissue microarrays were incubated with RPMC-FITC and TOPRO-3. Dual channel fluorescence microscopy shows that RPMC-FITC specifically binds to human colon adenocarcinoma. Scale bars: 15 μm.

ing affinity of RPMC-F or RPMC-DOTA for HT29 cells was 5 ± 1.9 nmol/L (χ^2, 0.986) and 6.4 nmol/L (χ^2, 0.944), respectively. When HT29 cells were incubated at 37°C for 1 hour with RPMC-F, the agent was rapidly internalized showing intracellular staining by confocal microscopy (Fig. 1*D*). When the incubations were carried out at 4°C, RPMC-F staining was limited to the cell surface (Fig. 1*E*), additionally confirming the internalization of RPMC-F. Importantly, the scrambled peptide control, REPC, containing the same amino acids but in different sequence, did not appreciably bind to HT29 cells (Fig. 1*C*). Screening of the peptide against tissue microarrays of human biopsies confirmed binding in all cancer samples tested (Fig. 1*F*) and showed absence of binding to normal tissues (Fig. 1*G*).

cDNA microarray analysis of colon cancer biopsy samples showed an up-regulation of fibronectin as compared with normal colon samples. Therefore, we decided to test the ability of RPMC-F to bind to fibronectin. Pretreatment of HT29 cells with human fibronectin almost completely inhibited binding of RPMC-F (92 ± 3%). However, peptide did not bind to fibronectin directly, suggesting that the binding partner is also a receptor for fibronectin. The integrin $\alpha_5\beta_1$ is a fibronectin binding partner that is also expressed by colon cancer cells. We were able to show that RPMC-F bound to purified $\alpha_5\beta_1$ integrin immobilized on Nunc Maxisorp plates with an average fluorescence of 61,116 ± 2,163 fluorescence units. In contrast, the $\alpha_5\beta_1$, well treated with scrambled control peptide REPC-F, had an average fluorescence of 576 ± 56 fluorescence units. Fluorescence-activated cell sorting analysis performed on HT29 cells incubated with RPMC-F or RPMC-F preincubated with $\alpha_5\beta_1$ showed the ability of the integrin to inhibit binding. RPMC-F labeled 98% of the HT29 cells, whereas RPMC-F preincubated with $\alpha_5\beta_1$ labeled only 52% of the cells examined under identical conditions.

***In vivo* Distribution and Pharmacokinetics.** To determine the *in vivo* behavior of the peptides, we injected tumor-bearing mice with RPMC-^{111}In-DOTA or with the scrambled control agent (REPC-^{111}InDOTA). Blood half-lives of the peptides were 24 and 21 minutes, respectively. High-performance liquid chromatography analysis confirmed that the peptides bound reversibly to serum proteins. Tumoral uptake of the RPMC-^{111}In-DOTA was 6.9% ID/g, >7-fold higher than the control peptide (1.1% ID/g; Fig. 2*A*). Furthermore, when ratios between tissue accumulation of RPMC versus control REPC were analyzed, it became apparent that there was an ~7-fold higher uptake in tumors with the RPMC peptide ($P < 0.01$). Ratios of normal tissues were close to 1, indicating no preferential distribution in other organs (Fig. 2*B*). At 24 hours after injection, biodistribution experiments showed that tumoral accumulation of RPMC-^{111}In-DOTA was 1.1% ID/g, whereas REPC-^{111}InDOTA was 0.48% ID/g. Activity in the kidneys was 4.0 and 4.9% ID/g for RPMC and REPC, respectively. All other tissues examined in Fig. 2 had activity levels < 0.1% ID/g. Tumoral accumulation of the RPMC peptide was specific because 98.4% of the activity could be competed by cold RPMC-DOTA. Gamma camera imaging in live mice confirmed that tumoral accumulation of the compound was sufficient for detection of implanted tumors (Fig. 2*C*). However, there was also considerable liver and renal activity, which is the reason we developed the affinity ligand for endoscopic detection of colon tumors.

Fluorescence Endoscopy. To determine whether colonic tumors could be detected in an orthotopic location by endoscopy, we used a fiberoptic microendoscope previously developed for examining colonic lesions in mouse models of colon cancer. As can be seen in Fig. 3, *A* and *B*, tumors were readily detectable by fluorescence microendoscopy after systemic injection of RPMC-F. Fluorescence measured by endoscopy performed 2 hours after injection showed the persistence of the agent in the tumor for prolonged periods of time. As anticipated from the biodistribution experiments, the control peptide failed to enhance tumors (Fig. 3, *C* and *D*). Fluorescence microscopy of frozen sections of these animals confirmed the macroscopic imaging findings (Fig. 3*E*). Taken together, these

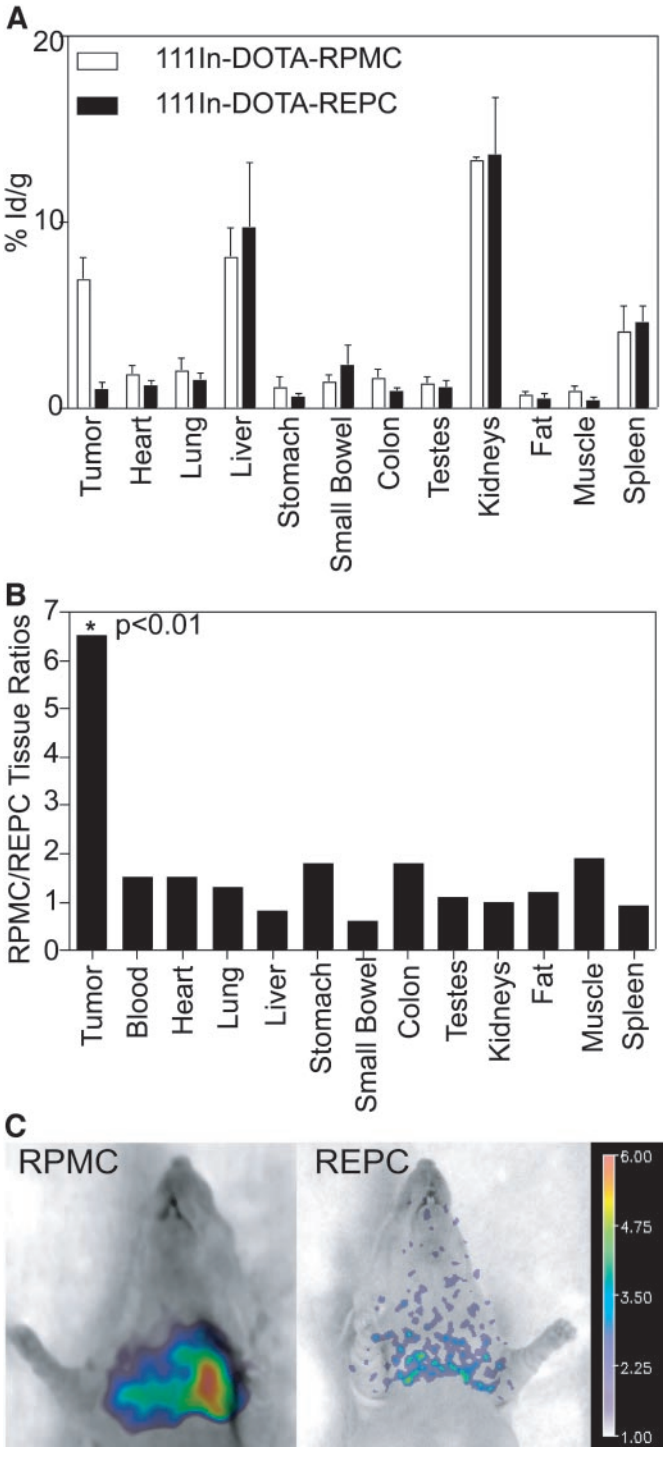

Fig. 2. Biodistribution of ^{111}In Dota-RPMC in mice. *A*. Nude mice bearing tumors derived from HT29 cells received injections of 100 uCi/200 μL of either ^{111}In Dota-RPMC or ^{111}In Dota-REPC peptide, and tissue radioactivity was measured 4 hours after injection. Results are expressed as %ID/g (mean ± SD, n = 4.5; *B*) ^{111}In Dota-RPMC to ^{111}In Dota-REPC tissue uptake ratio. Note the 7-fold higher accumulation of ^{111}In Dota-RPMC to ^{111}In Dota-REPC in tumor tissue, whereas all other tissues had equivalent accumulation of the two probes. *, $P < 0.01$ ^{111}In Dota-RPMC versus ^{111}In Dota-REPC. *C*, scintographic images of ^{111}In Dota-RPMC or the control overlayed onto white light images of tumor-bearing mice. Note the higher tumoral accumulation of ^{111}In Dota-RPMC.

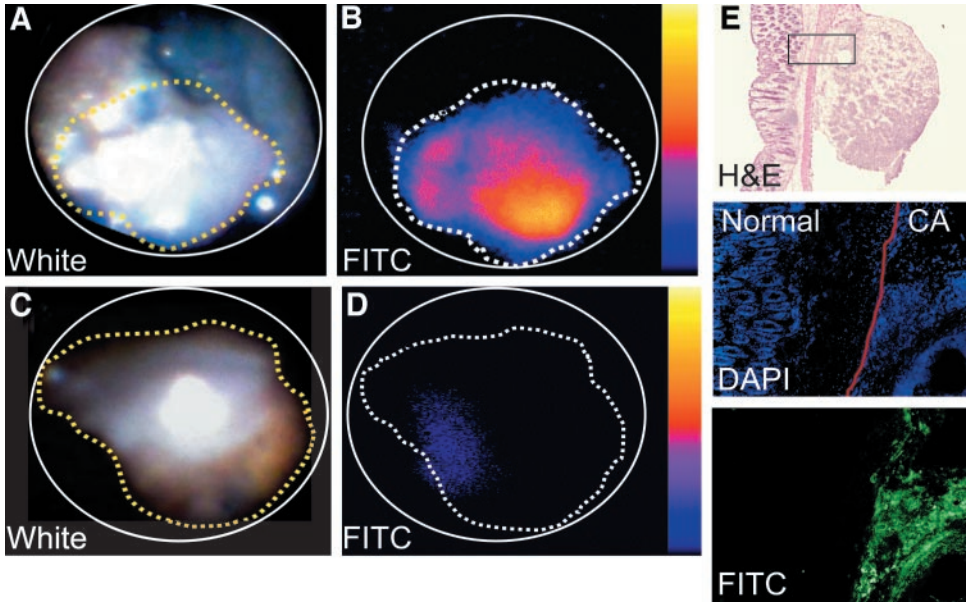

Fig. 3. Fluorescence endoscopy of animals with orthotopically implanted colon tumors. Anesthetized mice were examined by colonoscopy one hour after injection of RPMC-F (*A* and *B*) or the control REPC-F (*C* and *D*). Note the much higher fluorescence signal in the near-infrared channel for *B* than compared with *D* (control). *E*, serial sections of tumor from *A* showing an invasive growth pattern by H&E (top). Signal in the FITC channel originates exclusively from tumor on the right side because of accumulation of the RPMC-F peptide seen in bottom FITC channel.

data confirm the in vivo delivery and accumulation of RPMC-F but not REPC-F in colon tumors.

DISCUSSION

Detection of early colorectal cancers is essential for successful treatment. Although routine endoscopy is highly efficient in detecting adenomatous polyps, there exist instances in which cancers arise from nonpolypoid lesion or where there is an increased lifetime risk and repeated surveillance screening is necessary (6–9). In addition, there are instances in which it is desirable to detect local extension of tumor, accurately determine nodal involvement, or screen resection margins during surgical excision. For these circumstances, it would be beneficial to develop high-affinity optically detectable imaging agents. Unfortunately, such agents do not exist to date.

In the current research, we describe the systematic development and validation of a novel near-infrared fluorescence small molecule imaging agent targeted to colon cancer. Although several approaches exist for developing affinity ligands, we decided to start with an unbiased library approach that could subsequently be adapted to other cancers or investigations. Because the properties of targeted therapeutic and diagnostic imaging agents usually differ (e.g., single versus repeated injection, high target-to-background ratio versus therapeutic efficacy), we initiated a *de novo* screen. We determined that the following criteria for identification of peptides were essential properties of an effective screen. First, we decided to use a cylic rather than linear peptide to improve affinity for a specific partner. Second, the peptide should internalize, not remain cell surface bound, to maximize cellular trapping and increase local concentration (biological amplification). Third, the peptide should reversibly bind to plasma serum to prolong circulation and avoid rapid renal clearance. Finally, the peptide should be capable of accepting modifications for labeling with different fluorochromes or chelators while maintaining affinity.

We previously used differential phage display to identify the peptide consensus motif RPMC that binds specifically to human colon cancers (13). In the current study, we converted one of the lead sequences into a multifunctional imaging agent. This was done by COOH-terminal extensions and screening a number of preliminary compounds against tissue microarrays containing human colon cancers and normal tissue. We reasoned that because 85% of colorectal cancers arise from a pathway that involves chromosomal instability (1, 2), the probe would probably bind to a large percentage of colorectal tumors. Indeed, our colon cancer tissue microarray findings support this approach. Preliminary results suggest that the RPMC-F peptide may be binding to an integrin, specifically $\alpha_5\beta_1$ [a fibronectin binding partner (14, 15)], which is up-regulated in colon cancer (15). We are able to show that peptide binding to colon cancer cells could be inhibited by fibronectin. RPMC-F does not bind directly to fibronectin, however, suggesting that the peptide binds to a fibronectin binding partner. One such fibronectin binding partner expressed on colon cancer cells is $\alpha_5\beta_1$. In our experiments, RPMC-F bound to immobilized $\alpha_5\beta_1$ 100-fold greater than scrambled control peptide. Purified $\alpha_5\beta_1$ inhibited RPMC-F peptide binding to HT29 cells. The results from these two experiments suggest that $\alpha_5\beta_1$ is a binding partner of RPMC-F.

We then asked whether the lead candidate (RPMC-F) accumulated in ectopic and orthotopic colon cancers in a murine model. The lead peptide (containing radioactive indium chelated by a DOTA group) had a plasma half-life of 24 minutes, a similar half-life to a scrambled control peptide. Intravenous injection showed that the peptide accumulated to a significant amount in colon cancers (7-fold higher than control). Our results furthermore showed that the peptide was internalized into cancer cells and persisted intracellularly for several hours. Internalization and persistence are both highly desirable to assure adequate time during which the screening procedure can be done. Using a miniaturized fiber-optic approach, we successfully detected implanted colon cancers in mice and show that tumors were fluorescent for prolonged periods of time.

The mechanism exploited above for the development of optical tumor-specific imaging agents could have far reaching potential in cancer detection. In addition to the agent we describe here, alternative internalizing receptor systems [e.g., urokinase plasminogen activator receptors (16)] could also be explored for developing additional imaging agents with high tumor affinity. One could also envision a series of complementary fluorescent reagents that could be detected simultaneously in different wavelengths, such as the agent described here, combined with other optical reporters and sensors [e.g., for host response (17) and apoptosis (18) or angiogenesis detection agents (19)] to create a molecular imaging tumor profile. It is hoped that such molecular analysis will ultimately improve diagnosis, staging, and stratification of patients with colorectal cancer.

REFERENCES

1. Vogelstein B, Fearon ER, Hamilton SR, et al. Genetic alterations during colorectal-tumor development. N Engl J Med 1988;319:525–32.
2. Farber E, Rubin H. Cellular adaptation in the origin and development of cancer. Cancer Res 1991;51:2751–61.
3. Jemal A, Thomas A, Murray T, Thun M. Cancer statistics, 2002. CA - Cancer J Clin 2002;52:23–47.
4. Winawer SJ, Zauber AG, Ho MN, et al. Prevention of colorectal cancer by colonoscopic polypectomy. The National Polyp Study Workgroup. N Engl J Med 1993;329: 1977–81.
5. Rex DK, Cutler CS, Lemmel GT, et al. Colonoscopic miss rates of adenomas determined by back-to-back colonoscopies. Gastroenterology 1997;112:24–8.
6. Nakagoe T, Nanashima A, Sawai T, et al. Biological differences between polypoid and nonpolypoid growth types of colorectal cancer. Acta Med Nagasaki 2000;45: 53–9.
7. Rembacken BJ, Fujii T, Cairns A, et al. Flat and depressed colonic neoplasms: a prospective study of 1000 colonoscopies in the UK. Lancet 2000;355:1211–4.
8. Trowbridge B, Burt RW. Colorectal cancer screening. Surg Clin N Am 2002;82:943–57.
9. Krok K, Lichtenstein G. Colorectal cancer in inflammatory bowel disease. Curr Opin Gastroenterol 2004;20:43–8.
10. Funovics MA, Alencar H, Su HS, Khazaie K, Weissleder R, Mahmood U. Miniaturized multichannel near infrared endoscope for mouse imaging. Mol Imaging 2003; 2:350–7.
11. Marten K, Bremer C, Khazaie K, et al. Detection of dysplastic intestinal adenomas using enzyme-sensing molecular beacons in mice. Gastroenterology 2002;122:406–14.
12. Kelly K, Reynolds F, Weissleder R, Josephson L. FITC-hapten immunoassay: A versatile non-isotopic method for determining peptide-receptor interactions. Anal Biochem. In press 2004.
13. Kelly KA, Jones DA. Isolation of a colon tumor specific binding peptide using phage display selection. Neoplasia 2003;5:437–44.
14. Rajagopal S, Huang S, Albitar M, Chakrabarty S. Control of fibronectin receptor expression by fibronectin: antisense fibronectin RNA down-modulates the induction of fibronectin receptor by transforming growth factor beta1. J Cell Physiol 1997;170: 138–44.
15. Chiang HS, Peng HC, Huang TF. Characterization of integrin expression and regulation on SW-480 human colon adenocarcinoma cells and the effect of rhodostomin on basal and up-regulated tumor cell adhesion. Biochim Biophys Acta 1994;1224: 506–16.
16. Berger DH. Plasmin/plasminogen system in colorectal cancer. World J Surg 2002; 26:767–71.
17. Bremer C, Ntziachristos V, Weissleder R. Optical-based molecular imaging: contrast agents and potential medical applications. Eur Radiol 2003;13:231–43.
18. Petrovsky A, Schellenberger E, Josephson L, Weissleder R, Bogdanov A Jr. Near-infrared fluorescent imaging of tumor apoptosis. Cancer Res 2003;63: 1936–42.
19. Winter PM, Caruthers SD, Kassner A, et al. Molecular imaging of angiogenesis in nascent Vx-2 rabbit tumors using a novel alpha(nu)beta3-targeted nanoparticle and 1.5 tesla magnetic resonance imaging. Cancer Res 2003;63:5838–43.